Rapid Southern Ocean front transitions in an eddy-resolving ocean GCM

Andrew F. Thompson,[1] Peter H. Haynes,[1] Chris Wilson,[2] and Kelvin J. Richards[3]

Received 14 September 2010; revised 16 October 2010; accepted 19 October 2010; published XX Month 2010.

[1] The formation of persistent multiple fronts is an established feature of the Antarctic Circumpolar Current (ACC). Front strength and location are closely linked to eddy properties and therefore have important implications for the eddy-driven closure of the Southern Ocean meridional overturning circulation. ACC front structure is analyzed here by calculating regional probability density functions (PDFs) of potential vorticity diagnosed in an eddy-resolving ocean general circulation model. Rapid spatial transitions in the number of fronts and in the density classes over which they occur are found. Front transitions are associated with the major topographic obstacles Kerguelen Island, Campbell Plateau and Drake Passage; multiple fronts are preferentially found downstream of these features. These findings highlight the significant departure from zonal symmetry of the ACC front structure and emphasize the importance of local dynamics on large-scale Southern Ocean properties.
Citation: Thompson, A. F., P. H. Haynes, C. Wilson, and K. J. Richards (2010), Rapid Southern Ocean front transitions in an eddy-resolving ocean GCM, *Geophys. Res. Lett.*, *37*, LXXXXX, doi:10.1029/2010GL045386.

1. Introduction

[2] Water mass properties in the Antarctic Circumpolar Current (ACC) are observed to be concentrated in multiple fronts [e.g., *Sokolov and Rintoul*, 2009]. These fronts are often collocated with strong zonal jets, similar to examples in other geophysical contexts [see *Baldwin et al.*, 2007, and references therein], including the Earth's atmospheric jet stream and multiple jets in large planetary atmospheres. In all of these examples, the formation of fronts and jets arises from interaction between eddies and mean flow and implies a strong spatial variation of eddy transports. In the ACC eddy transport plays a major role in the dynamics of the Southern Ocean meridional overturning circulation (MOC), which influences water mass formation, meridional heat transport and carbon dioxide uptake. Variations in eddy transport thus have important implications for the MOC and hence the global climate system.

[3] Potential vorticity (PV) is widely accepted as a valuable dynamical diagnostic in a large class of geophysical flows. In the ocean PV is materially conserved along isopycnals in the absence of frictional processes or diapycnal mixing, which are generally weak in the interior of the ACC. PV distributions, as that of any materially conserved scalar, therefore encodes important information about eddy transport. In other applications, such as transport of stratospheric chemical species [*Sparling*, 2000], probability density functions (PDFs) have been used as an effective means of describing spatial variations and identifying important features. Indeed, *Marshall et al.* [1993] used PDFs to demonstrate PV homogenization in a simple dynamical model of the ACC and with a coarse resolution hydrographic data set.

[4] A feature of the Southern Ocean that distinguishes it from the atmosphere is the fronts' strong departure from zonal symmetry. *Sokolov and Rintoul* [2007, 2009] used satellite altimetry to identify as many as twelve ACC fronts that undergo persistent merger and divergence events and modulations in intensity along the path of the ACC. *Shuckburgh et al.* [2009] used velocity fields derived from satellite altimetry to advect a passive tracer and calculate an effective diffusivity [*Nakamura*, 1996] over local "patches" of the ACC. Effective diffusivity profiles differed between patches providing evidence for mixing variations along the path of the ACC. This paper goes beyond these previous studies by analyzing, using PDFs of PV, the ACC's multiple front structure, as manifested in *subsurface* PV distributions, and by identifying sharp zonal transitions. By summarizing large amounts of data efficiently, PDFs of PV can provide an excellent tool for detecting both horizontal and vertical transitions in front structure and for indicating key regions that have a dynamical influence on the MOC.

2. Data and Methods

[5] The temporal and spatial distribution of PV, $q = \rho^{-1}(f + \zeta)\partial\sigma_2/\partial z$, is calculated using numerical output from the 1/10 degree OfES primitive equation model (Ocean General Circulation Model for the Earth Simulator) [*Masumoto et al.*, 2004] and interpolated onto isopycnal surfaces. Here f is the Coriolis frequency, $\zeta = u_y - v_x$ is relative vorticity, σ_2 is potential density referenced to 2000 m (units of kg m^{-3} understood) and ρ is *in situ* density. OfES includes 54 vertical levels with a realistic bathymetry. The model has high spatial and temporal resolution and solves a dynamically consistent set of equations relevant to the Southern Ocean. Our approach is to regard this as a useful surrogate for the real Southern Ocean. In fact, the PV distributions extracted from OfES are broadly similar to those generated from the Southern Ocean State Estimate (SOSE) model [*Mazloff et al.*, 2010], which has a coarser resolution (1/6 degree), but includes data assimilation.

[6] Construction of a reliable PDF requires a sufficiently large number of data points. Our approach is to use a single snapshot of the PV field, but calculate PDFs from a sam-

[1]Department of Applied Mathematics and Theoretical Physics, University of Cambridge, Cambridge, UK.
[2]National Oceanography Centre, Liverpool, UK.
[3]School of Ocean and Earth Science and Technology, University of Hawaii at Manoa, Honolulu, Hawaii, USA.

0094-8276/10/2010GL045386

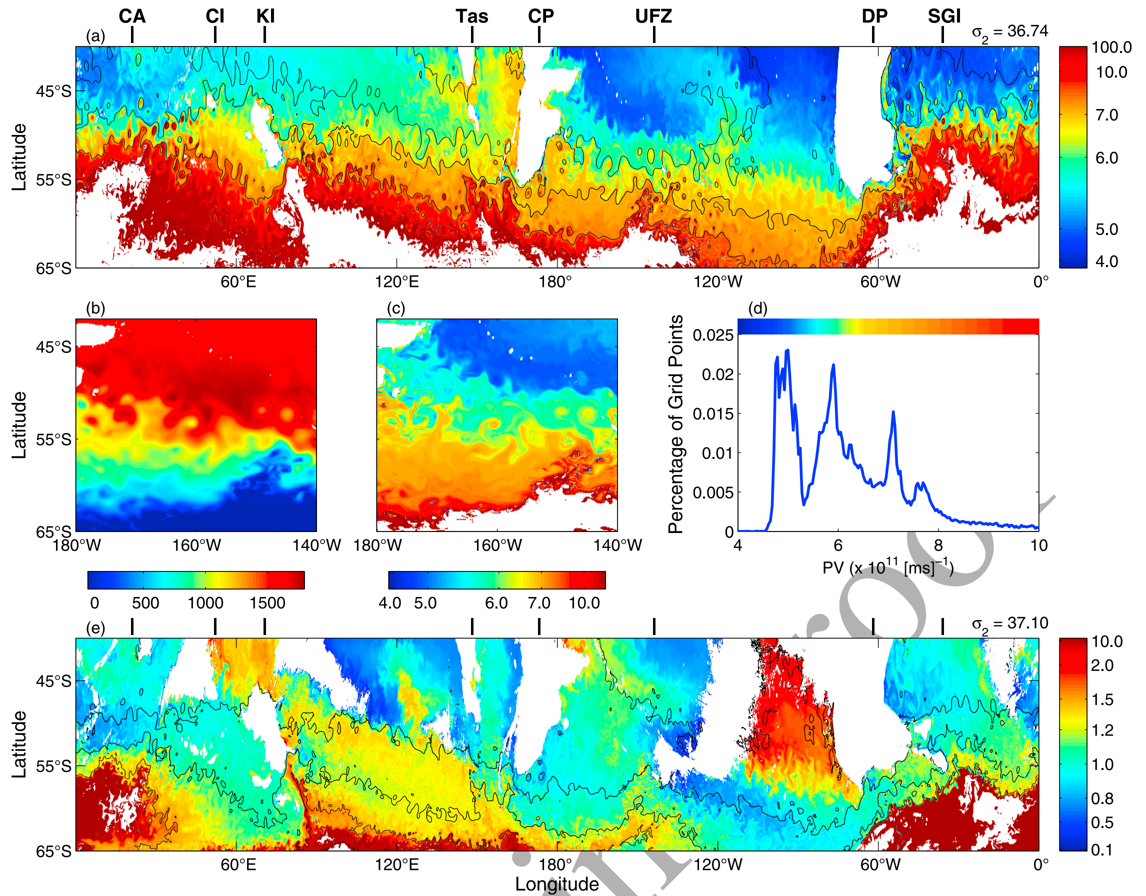

Figure 1. (a) Snapshot of potential vorticity PV ($\times 10^{-11}$ [ms]$^{-1}$) on the $\sigma_2 = 36.74$ potential density surface in the Southern Ocean of the eddy-resolving OfES model. Land and isopycnal depths shallower than 100 m are colored white. Contours indicate isopycnal depth, with the 500, 1000 and 1500 m isolines plotted. (b) Isopycnal depth (m) over the region 180°W to 140°W and (c) an expanded view of PV in this region. (d) Probability density function of PV values in Figure 1c, normalized by the mean PV; the non-linear colorscale in Figures 1a and 1c is mapped onto the abscissa. (e) Snapshot of PV on the $\sigma_2 = 37.10$ potential density surface. Contours indicate the 1000, 2000 and 3000 m isolines of isopycnal depth. Markers above Figure 1a indicate key topographical features: CA, Cape Agulhas; CI, Crozet Island; KI, Kerguelen Island; Tas, Tasmania; CP, Campbell Plateau; UFZ, Udintsev Fracture Zone; DP, Drake Passage; SGI, South Georgia Island.

pling region with finite zonal width. Choosing this width as 10° was found to be large enough to give robust PDFs and small enough to show significant zonal variation. The sampling regions span 65°S to 40°S and were further required to contain at least 2000 grid points. Temporal variability is discussed below.

3. Results

[7] Figure 1a shows a typical snapshot of PV on the $\sigma_2 =$ 36.74 potential density surface with land masses and fluid at a depth less than 100 m colored white. The PV distribution is dominated by a large-scale gradient, but mesoscale eddies give rise to regions of sharper and weaker PV gradients. A region of particularly well-defined fronts is found downstream of the Campbell Plateau (CP) between 180°W and 140°W (Figures 1b and 1c). Figure 1d displays a PDF of PV over the region in Figure 1c, normalized by the mean PV in this region; the non-linear color scale in Figures 1a and 1c is mapped to the abscissa. PV is found in four distinct pools (PDF maxima) separated by three fronts (PDF minima). At greater depths the influence of topography becomes stronger, as shown by a snapshot of PV along the $\sigma_2 = 37.10$ potential density surface (Figure 1e). Here topographic obstacles may shield and isolate regions of the ACC, which induce significant regional variability in the meridional PV gradient. Indeed, reversals in the sign of the large-scale PV gradient occur at 30°E, 80°E, 120°W, and 60°W. As linear instability properties of the ACC depend on the vertical structure of meridional PV gradient [*Smith and Marshall*, 2009], variations in this gradient will have important implications for regional differences in eddy characteristics along the path of the ACC.

[8] In Figure 1d, a line plot PDF of PV is calculated over a sampling region on an isopycnal surface. By slowly changing the mean longitude/isopycnal of the window (now using a 10° zonal extent), horizontal/vertical variations in the front structure can be identified. Figure 2 shows the accumulation of PDF line plots on the $\sigma_2 = 36.36$ (Figure 2a), $\sigma_2 = 36.74$ (Figure 2b) and $\sigma_2 = 37.10$ (Figure 2c) density surfaces as the sampling region is shifted along the path of the ACC. Warm colors indicate high probability of the corresponding PV value on the ordinate; the thin black curves mark local maxima of the individual PDFs (cf.

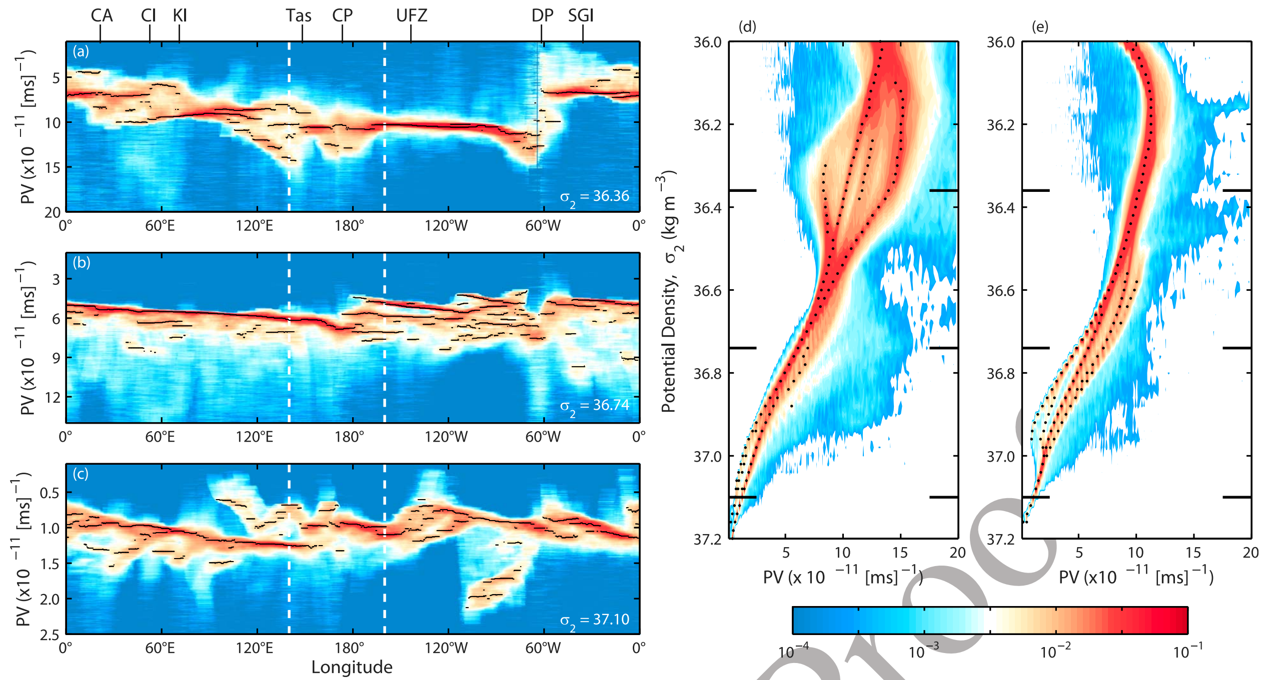

Figure 2. Probability density function (PDF) of potential vorticity (PV) as a function of longitude on the (a) σ_2 = 36.36, (b) σ_2 = 36.74 and (c) σ_2 = 37.10 potential density surfaces. The PDFs are normalized by the mean PV in each window (see text for full discussion). The thin black lines mark local maxima of the individual PDFs. The full vertical extent of the PDFs along the white dashed lines is (d) 140°E and (e) 160°W. The black lines correspond to the isopycnals in Figures 2a–2c and the black dots mark local maxima of the individual PDFs. Markers showing the position of key topographical features are defined in the caption of Figure 1.

Figure 3). Figures 2d and 2e show the accumulation of PDF line plots on different isopycnals at the longitudes indicated by the dashed lines in Figures 2a–2c. Again, warm colors indicate PDF maxima, corresponding to regions of homogenized PV. Major topographical features are marked along the top of Figure 2a for reference.

[9] PV front structure varies significantly both along the path of the ACC and in the vertical. In particular, Figure 2a shows distinct partitioning of PV along the σ_2 = 36.36 isopycnal. Immediately downstream of Kerguelen Island (KI, 70°E) PV has a largely uniform value around 10 × 10^{-11} m^{-1} s^{-1}, which may be related to mixing occurring

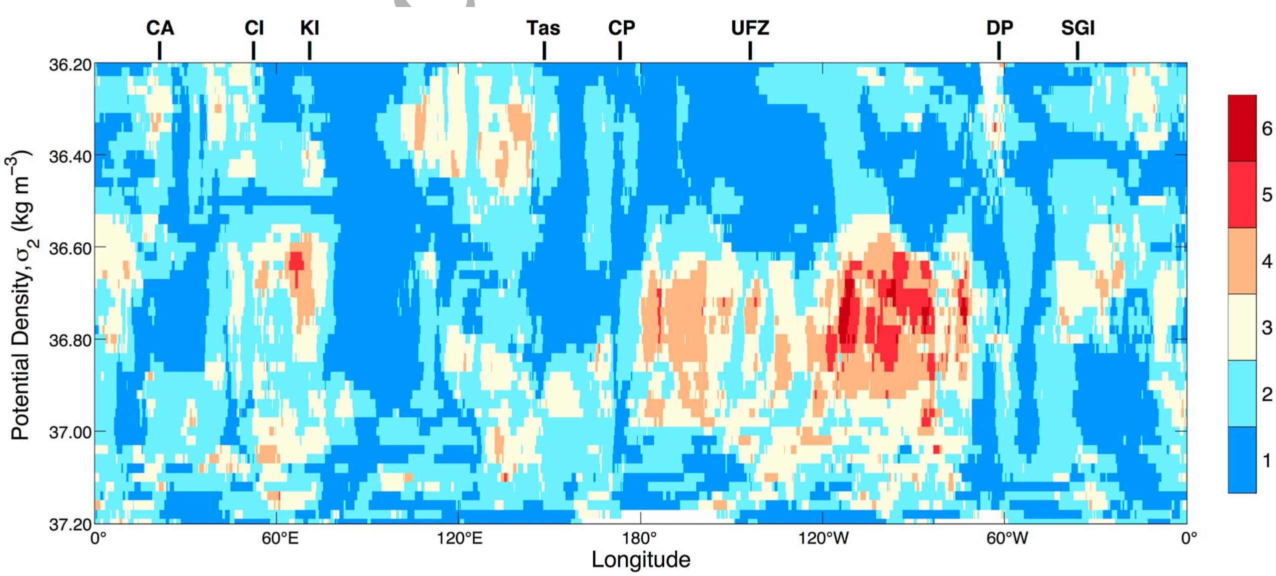

Figure 3. Number of distinct homogenized pools of potential vorticity (PV) as a function of longitude and potential density surface. Distinct PV pools are determined by the number of local maxima in a probability density function (PDF) of PV on a given isopycnal surface spanning 10° longitude and 25° latitude. Large values are indicative of multiple fronts. Markers showing the position of key topographical features are defined in the caption of Figure 1.

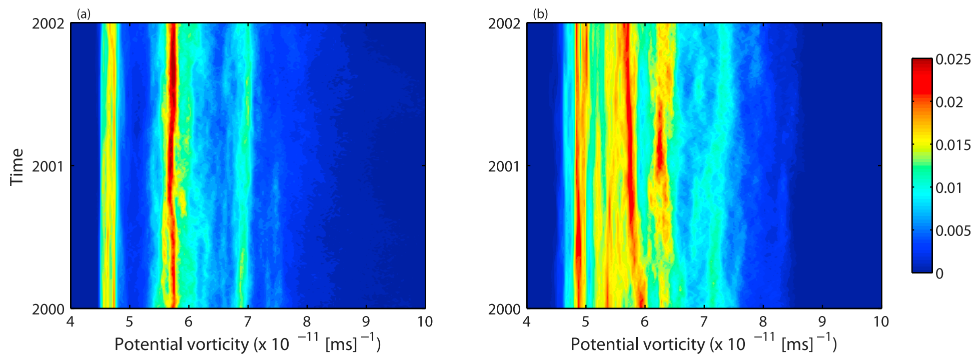

Figure 4. Two year evolutions of PV PDFs over the regions (a) 180°W to 140°W (Figure 1c) and (b) 120°W to 80°W on the σ_2 = 36.74 isopycnal.

over and around this large topographic obstacle. Further downstream in the Indian Sector, three to four distinct fronts occur that are associated with the northern flank of the ACC and a zonally-oriented ridge south of Australia. On this shallow isopycnal, PV is largely uniform over the Pacific sector of the ACC, consistent with PV homogenization in the South Pacific gyre circulation [*Marshall et al.*, 1993]. A rapid change in the outcropping latitude of this isopycnal through Drake Passage (DP) contributes to the step-like transition in PV near 60°W. Multiple fronts found south of Cape Agulhas (CA, 20°E) reflect contributions from the core of the ACC as well as from the Agulhas retroflection. Along the σ_2 = 36.74 isopycnal (Figure 2b), multiple distinct PV pools are found in the Pacific sector, particularly above the abyssal plains downstream of the Udintsev Fracture Zone (UFZ, 145°W). On this particular isopycnal the signature of multiple fronts is much weaker downstream of KI. PV structure along σ_2 = 37.10 (Figure 2c) is strongly constrained by topography as suggested by Figure 1e. Isolated patches of PV can lead to abrupt changes in the meridional PV distribution, e.g., the low PV values near 100°E and the large PV values near 90°W.

[10] Vertical transitions in PV structure also exhibit regional differences. In the Indian sector (Figure 2d), distinct PV pools are found within the density class $36.1 < \sigma_2 < 36.5$, associated with the northern boundary of the ACC. These collapse to nearly uniform PV along the σ_2 = 36.6 isopycnal surface, which is reflected in a weak PV gradient on this isopycnal. Distinct pools of homogenized PV are then found at deeper isopycnals. In the Pacific sector (Figure 2e), PV is largely homogeneous on isopycnals where $\sigma_2 < 36.5$, as discussed above. On deeper isopycnals, three to four distinct PV pools are found as indicated by the black dots.

[11] The particular isopycnals and longitudes displayed in Figure 2 are representative of the different horizontal and vertical variability apparent in the PV structure. However, these individual "running" PDFs do not provide a comprehensive view of PV front characteristics. In Figure 3 the information from the PDFs is collapsed into a single plot by calculating the number of independent maxima from each of the windowed PV PDFs, e.g., the black curves and black dots in Figure 2. A relatively crude method is employed to count the maxima: to qualify, a local maxima must be a threshold value greater than both neighboring local minima. Figure 3 uses a threshold value of 0.0025, although the qualitative pattern that emerges is largely insensitive to the threshold value. Thus Figure 3 shows the number of maxima, or distinct pools of PV, as a function of longitude and isopycnal surface (PDFs are still calculated using a 10° zonal extent).

[12] Figure 3 shows clear transitions in front structure at the major topographical obstructions KI, CP and DP. Interpretation of this plot requires care because, as seen in Figure 1, isopycnal surfaces may span a large depth range across the ACC, and different density classes may be found in the core of the ACC in different locations. PV on shallow isopycnals on the northern flank of the ACC appears to be homogenized throughout much of the Southern Ocean with the exception of the region downstream of KI. The isopycnal surface σ_2 = 36.50 appears here as a surface of uniformly small number of peaks, and is the lower boundary of the shallow homogenized PV region in the Pacific sector. In the Indian sector of the ACC (~120°E), multiple fronts are found in two different density classes, reflecting front formation on both flanks of the ACC, whereas in the Pacific sector (~120°W) there is only a single density class exhibiting multiple fronts. There is some evidence of multiple fronts in two density classes in the Atlantic sector, however the transition is found at shallower isopycnals than in the Indian sector. The major topographical features are also associated with a reduction in the number of fronts near or just downstream of the obstruction.

[13] Temporal variability of the PDFs of PV is, to a degree, spatially dependent. Front structure associated with topographically-constrained jets is largely stationary, as in Figure 4a, which shows the time evolution of the PV PDF corresponding to the region in Figure 1c. On the same isopycnal (σ_2 = 36.74) in the eastern Pacific sector, where topography is relatively flat, the amplitude and location of the PDF maxima are more variable (Figure 4b), which may arise from either forcing variability or internal variability. Still, the number of distinct PV fronts remains largely constant over this period. This, then, supports the assertion that snapshots, like Figure 3, provide a useful representation of the longer term front structure, certainly on time scales of many months.

4. Discussion

[14] Complicated eddy processes in the ACC influence global climate through their effect on the MOC and are manifest in a complex structure of jets and fronts. Here we have resolved the spatial (and to an extent temporal) variability of the ACC's front structure by employing a novel

diagnostic, calculating PDFs of PV on isopycnals, applied to a high resolution ocean GCM. The results show that PV fronts form in specific regions of the ACC and on specific density classes. Rapid alongstream transitions between these regions are detected for the first time. The significant vertical and alongstream variability of the front structure is consistent with the spatially-dependent mixing described by *Shuckburgh et al.* [2009] and *Abernathy et al.* [2010], but here identification of sharp changes in front structure point to regions that are likely to exert dynamical control over the MOC and merit further study.

[15] PDFs are an efficient means of analyzing a large amount of complicated data. Because of this, it can be difficult to determine with certainty the physical processes responsible for the observed transitions in front structure. Still, the correlation between front transitions and topographical features is remarkable. Topography acts to both steer mean flows and modify PV gradients, and these changes may feed back on eddy generation through barotropic and baroclinic instabilities [*Thompson*, 2010], leading to enhanced mixing. Figure 3 shows evidence of these local dynamical processes as immediately downstream of the major topographical constrictions KI, CP and DP there is a full-depth reduction in the number of homogenized pools of PV. We note that topographical features also tend to be sites of internal wave generation that can enhance diapycnal mixing and modify interior PV. It is not well known at present how vertical mixing impacts front structure. Finally, topography may also alter PV distributions through modifications in stratification related to rapid changes in isopycnals that outcrop or in outcrop locations; this is especially evident across Drake Passage (Figures 2 and 3). Besides being a key sink of momentum input by surface winds, these results indicate that topography also (i) acts as a catalyst for local re-organization of water mass structure and (ii) isolates regions of the deep ACC, which affects large-scale PV gradients.

[16] This study begins to link the work of *Shuckburgh et al.* [2009] and *Abernathy et al.* [2010] with *Sokolov and Rintoul* [2007, 2009]. Multiple jets are found throughout the ACC, but the effectiveness of these jets acting as barriers to transport (i.e., to separate distinct water masses) likely varies along the path of the ACC. Specifically, this study highlights the need to further study the dynamical relationship between fronts and velocity jets in the ACC, including the link between surface fronts and interior PV distributions. Indeed, although *Sokolov and Rintoul* [2009] identify many circumpolar fronts from altimetry data, *Shuckburgh et al.* [2009] discover a much smaller number of low mixing regions in certain parts of the ACC using the same data set. This study also indicates that changes in transport properties may occur rapidly and may depend on local dynamics, such as constraints on the flow past topography. This suggests that local dynamics impact global properties of the Southern Ocean and its MOC, and care must be taken in the interpretation of regional observations or of zonally-averaged theories of Southern Ocean circulation.

[17] The most striking result of this study is the strong zonal variation and the dominant control of topography over the ACC's multiple front structure. This behavior motivates a possible model of the ACC that is comprised of zonally-uniform regions separated by sharp transitions. The physical processes that govern the rapid re-organization of the front structure at these topographical transition zones is the focus of on-going research.

[18] **Acknowledgments.** The authors gratefully acknowledge the provision of OfES output by Hideharu Sasaki and James Potemra. We also thank Matt Mazloff for supplying SOSE output. AFT was supported by NERC, NE/E013171/1. CW was supported by NERC through Oceans 2025 and NE/I001794/1.

References

Abernathy, R., J. Marshall, M. Mazloff, and E. Shuckburgh (2010), Enhanced isopycnal mixing at steering levels in the Southern Ocean, *J. Phys. Oceanogr.*, *40*, 170–184.

Baldwin, M. P., P. B. Rhines, H.-P. Huang, and M. E. McIntyre (2007), The jet-stream conundrum, *Science*, *315*, 467–468.

Marshall, J., D. Olbers, H. Ross, and D. Wolf-Gladrow (1993), Potential vorticity constraints on the dynamics and hydrography of the Southern Ocean, *J. Phys. Oceanogr.*, *23*, 465–487.

Masumoto, Y., et al. (2004), A fifty-year eddy-resolving simulation of the World Ocean—Preliminary outcomes of OFES (OGCM for the Earth Simulator), *J. Earth Simulat.*, *1*, 35–56.

Mazloff, M. R., P. Heimbach, and C. Wunsch (2010), An eddy-permitting Southern Ocean State Estimate, *J. Phys. Oceanogr.*, *40*, 880–899.

Nakamura, N. (1996), Two-dimensional mixing, edge formation, and permeability diagnosed in area coordinates, *J. Atmos. Sci.*, *53*, 1524–1537.

Shuckburgh, E., H. Jones, J. Marshall, and C. Hill (2009), Understanding the regional variability of eddy difusivity in the Pacific sector of the Southern Ocean, *J. Phys. Oceanogr.*, *39*, 2011–2023.

Smith, K. S., and J. Marshall (2009), Evidence for enhanced eddy mixing at middepth in the Southern Ocean, *J. Phys. Oceanogr.*, *39*, 50–69.

Sokolov, S., and S. R. Rintoul (2007), Multiple jets of the Antarctic Circumpolar Current south of Australia, *J. Phys. Oceanogr.*, *37*, 1394–1412.

Sokolov, S., and S. R. Rintoul (2009), Circumpolar structure and distribution of the Antarctic Circumpolar Current fronts: 1. Mean circumpolar paths, *J. Geophys. Res.*, *114*, C11018, doi:10.1029/2008JC005108.

Sparling, L. C. (2000) Statistical perspectives on stratospheric transport, *Rev. Geophys.*, *38*, 417–436.

Thompson, A. F. (2010), Jet formation and evolution in baroclinic turbulence with simple topography, *J. Phys. Oceanogr.*, *40*, 257–278.

P. H. Haynes and A. F. Thompson, Department of Applied Mathematics and Theoretical Physics, Centre for Mathematical Sciences, University of Cambridge, Wilberforce Road, Cambridge CB3 0WA, UK. (a.f.thompson@damtp.cam.ac.uk)

K. J. Richards, School of Ocean and Earth Science and Technology, University of Hawaii at Manoa, 1680 East West Rd., Honolulu, HI 96822, USA.

C. Wilson, National Oceanography Centre, 6 Brownlow St., Liverpool L3 5DA, UK.